

# Investigation of Energy Dissipation in an Ejector Refrigeration Cycle

Christian Tischendorf<sup>1</sup> Denise Janotte<sup>2</sup> Ricardo Fiorenzano<sup>1</sup> Wilhelm Tegethoff<sup>2</sup>

<sup>1</sup> Technical University Braunschweig, Department of Thermodynamics

<sup>2</sup> TLK Thermo GmbH

Hans-Sommer-Straße 5, 38106 Braunschweig Germany

c.tischendorf@tu-bs.de

## Abstract

The presented work focuses on the differences in energy dissipation in each cycle component compared to the energy dissipation of the whole ejector refrigeration cycle. With help of this analysis, improvement of energetic efficiency by using an ejector can be set in relation to the potential improvement in efficiency of other components such as heat exchangers. Information about entropy production associated with energy dissipation allows for an objective estimation of the optimization potential of each component within an ejector refrigeration cycle. In addition, the improvement due to the specific process control of the ejector cycle compared to the conventional heat pump cycle can be analyzed. The energetic benefit gained using an ejector depends on the refrigerant used. The refrigerants R134a and R744 (CO<sub>2</sub>) were compared in regard to the entropy production of the heat pump system.

In order to simulate an ejector refrigerant cycle and to evaluate the energy dissipation by means of entropy production, existing models for cycle components were modified. Applying the second law of thermodynamics, local distribution of entropy production as well as the overall entropy produced in each component was determined. The analysis showed that entropy production is caused by two types of effects. One part results from real effects such as pressure drop and heat transfer, the other part is due to the modeling assumptions made. Thus, the investigation of energy dissipation leads to a deeper understanding of the model.

The simulated amount of entropy produced is summarized in a record, so that the results can be read easily by other programs, e.g. programs that visualize energy and entropy flows. In the presented investigation the entropy flow and dissipation effects were analyzed by means of diagrams, such as Sankey diagrams.

The complete heat pump system has been simulated

using the Modelica library TIL (TLK-IFT-Library) in order to determine the energy dissipation in each cycle component. With the modified TIL models, other process controls can also be investigated. This approach offers the opportunity to analyze the energy dissipation in detail, and differs in that sense from the commonly used technique of integrated energy balances and COP determinations.

*Keywords:* entropy analysis; refrigeration; compression cycle; simulation; CO<sub>2</sub>; R134a

## 1 Introduction

The pressure difference between the high and low pressures in CO<sub>2</sub> refrigerant systems is high compared to other refrigerants, e.g. R134a. Previous investigations by other authors have shown that in a conventional refrigeration cycle, the pressure differences cause significant throttling losses. Using an expansion valve results in an isenthalpic throttling process, which means that the kinetic energy is completely dissipated and the evaporation enthalpy is reduced compared to an isentropic process.

Using an ejector is one way to recover part of the lost kinetic energy and to increase refrigeration capacity. As a result, the energetic efficiency (COP) of the refrigerant system will be improved. In addition to the improvement caused by an ejector, the COP can be raised by optimization of other cycle components. The key issues are the comparative cost effectiveness of the modifications, as well as the question of which components have the most optimization potential. Therefore, an analytical technique enabling one to recognize optimization potential is needed in order to assess the alternative solutions. The required technique was developed during the project presented in this work.

One approach to investigate the potential is to ap-

ply the second law of thermodynamics to determine the produced entropy in each refrigeration cycle component, so that a basic analysis of the component efficiencies is possible. This approach was introduced in [Franke04]. In the presented work, the investigation was carried out using the Modelica library TIL to simulate the refrigeration cycles. TIL is a component library for steady-state and transient simulation of fluid systems such as heat pump, air conditioning, refrigeration or cooling systems, developed by TLK-Thermo GmbH and TU Braunschweig, Institute for Thermodynamics [for a detailed description see [Richter08]]. The advantage of TIL is that it has a very shallow inheritance structure, which makes the models easy to understand and extend. The results of the entropy analysis were visualized by bar and Sankey charts using the newly developed software EnergyViewer by TLK-Thermo GmbH, in order to simplify the interpretation of the effects.

## 2 Simulated Refrigeration Cycle

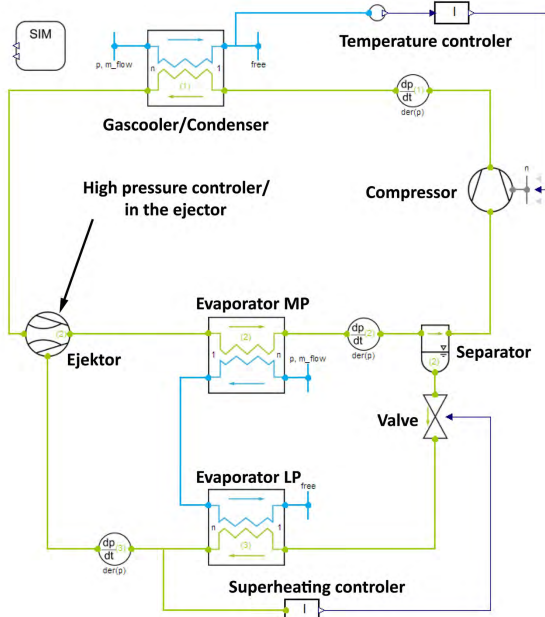


Figure 1: Object diagram of the simulated cycle

In the presented work, an ejector heat pump used for heating water for domestic use and floor heating using R744 or R134a as refrigerant was simulated. The principal functionality of a common ejector refrigerant cycle is described in the following literature [Elbel06]. For this investigation, the common ejector refrigeration cycle was modified. An object diagram of the modified ejector refrigeration cycle is

shown in figure 1. The cycle consists of the following components: gas cooler (R744)/ condenser (R134a), medium pressure evaporator (MP), low pressure evaporator (LP), valve, separator, compressor and ejector. In addition, a temperature controller and a super-heating controller were added in the cycle. As well, a high pressure controller was added to the ejector component model. The heat pumps were simulated at the following conditions.

**heating capacity for both operation modes:**

5000 W

**temperature floor heating water:**

30 °C to 35 °C

**temperature domestic hot water:**

10 °C to 60 °C

**overall heat transfer capability gas cooler/condenser:**

1400 W/K

**overall heat transfer capability evaporator LP/MP:**

500 W/K

**heat exchanger pressure drop R744 refrigerant:**

1 bar

**heat exchanger pressure drop R134a refrigerant:**

0,2 bar

**water mass flow rate evaporator**

equal for all simulations

**water temperature of heat source**

10 °C

**high pressure**

set to optimize the conditions in the gas cooler/condenser (low mean driving temperature difference)

The water that serves as a heat source first flows through the evaporator MP and afterward through the evaporator LP. The temperature controller controls the speed of the compressor, such that the desired output temperature is achieved by a constant water mass flow rate through the gas cooler or condenser. The controller integrated in the ejector controls the high pressure level by setting the mass flow rate through the driving nozzle. The controller determines a high pressure level, which can be adjusted such that optimal conditions are found in the gas cooler or condenser. The super-heating controller is used to create optimal conditions in the evaporator LP.

## 3 Effects Causing Entropy Production in the Cycle Components

An important distinction must be made between entropy production caused by numerical errors based on

modeling assumptions and the entropy produced due to real physical effects. The numerical errors depend on the mathematical model as well as on the degree of discretization when using a discretized model. The real physical effects depend on the quality and the construction of the refrigeration cycle components and can be influenced by the specific process control. In addition to this, the produced entropy is dependent on the refrigerant used. In the presented work the following entropy producing effects generated in the cycle components were investigated:

- **Heat Exchanger**  
pressure drop, heat transfer and numerical errors (modeling)
- **Valve**  
pressure drop (isenthalpic expansion)
- **Compressor**  
efficiency based model
- **Ejector**  
special efficiency based model
- **Separator**  
mixing effects

### 3.1 Heat Exchanger

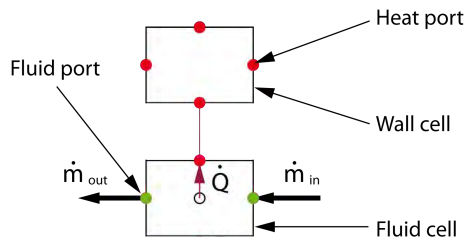


Figure 2: Illustration of cell structure of a tube

The heat exchangers used for the investigation consist of tubes connected via heat ports. The number of tubes and the direction in which the medium flows through them can vary. The manner of connection specifies the kind of heat exchanger. For this paper, counterflow heat exchangers consisting of one liquid and one refrigerant tube were used. The medium used in the liquid tube was water. The tubes are divided into cells, and each tube is comprised of two types of cells: wall cells and fluid cells (see figure 2). The fluid cells can be either liquid or refrigerant cells, depending on the type of medium flowing through them. The connection of fluid and wall cells via heat ports allows the exchange of heat between the cells. The temperature of the connected heat ports of two cells are set

equal. The heat transfer inside the cell between the medium and the heat port is determined by the heat transfer relation and the heat transfer coefficient. In the cell model, equations to determine the heat flow are implemented. A similar modeling of heat transfer and fluid flow is presented in [Patankar80]. The number of wall and fluid cells in each tube determines the degree of discretization (finite volume approach). An introduction to the finite volume approach can be found in [Baumann06]. In order to model the entropy production within the heat exchangers, a hierarchical approach was followed. First the entropy production due to the aforementioned effects was determined for each cell of the heat exchanger. The second law of thermodynamics for a transient system yields:

$$\frac{d(sm)}{dt} = \sum_{i=1}^n \dot{m}_i s_i + \dot{S}_Q + \dot{S}_{prod}^Q + \dot{S}_{prod}^{\Delta p} + \dot{S}_{prod}^M \quad (1)$$

With  $\frac{d(sm)}{dt}$  being the change of entropy of the cell. The terms  $\sum_{i=1}^n \dot{m}_i s_i$  and  $\dot{S}_Q$  specify the entropy conveyed by mass and heat flows.  $\dot{S}_{prod}^Q$ ,  $\dot{S}_{prod}^{\Delta p}$ ,  $\dot{S}_{prod}^M$  represent the entropy production rate due to heat transfer, pressure drop and modeling respectively. Heat transfer and pressure drop are real effects that cause entropy production, which can be determined by formulas presented later. The last production term, however, is due to the modeling of the cell as a volume with constant medium properties such as enthalpy or temperature. For a **fluid cell** this can be illustrated by the image of an agitator stirring the medium inside the cell so that it is perfectly mixed. Because of the modeling assumptions, the enthalpy of the medium inside the cell matches the enthalpy at the outlet port of the cell. Likewise, the temperature of the medium inside the cell matches the temperature at the outlet port of the cell. If there is a temperature change, this mixing of the cell content produces entropy. This entropy production  $\dot{S}_{prod}^M$  is numerical error and differs from  $\dot{S}_{prod}^{Mi,T}$  the entropy production due to mixing of two streams of ideal gas  $\dot{m}_a$  and  $\dot{m}_b$  with temperature  $T_a$  and  $T_b$  respectively which is presented in [Cerbe07] as follows:

$$\dot{S}_{prod}^{Mi,T} = \dot{m}_a c_{ma} \Big|_{T_a}^{T_{Mi}} \ln \frac{T_{Mi}}{T_a} + \dot{m}_b c_{mb} \Big|_{T_b}^{T_{Mi}} \ln \frac{T_{Mi}}{T_b} \quad (2)$$

with  $T_{Mi}$  being the mixing temperature and  $c_m$  the mean specific heat capacity of stream a or b. Hence  $\dot{S}_{prod}^M$  has to be determined via the second law. Transforming equation 1 and setting  $\frac{dm}{dt} = \sum_{i=1}^n \dot{m}_i$  yields:

$$\dot{S}_{prod}^M = m \frac{ds}{dt} - \sum_{i=1}^n \dot{m}_i (s_i - s) - \dot{S}_Q - \dot{S}_{prod}^Q - \dot{S}_{prod}^{\Delta p} \quad (3)$$

The index  $i$  labels the variables of stream  $i$  flowing in or out of the cell. The variables of the medium inside the cell do not have index labels. Each fluid cell has only one inlet  $\dot{m}_{in}$  and one outlet stream  $\dot{m}_{out}$ . The modeling assumption yields  $s = s_{out}$  so that the equation can be simplified further.

$$\dot{S}_{prod}^M = m \frac{ds}{dt} - \dot{m}_{in} (s_{in} - s) - \dot{S}_Q - \dot{S}_{prod}^Q - \dot{S}_{prod}^{\Delta p} \quad (4)$$

Without heat transfer and pressure drop, there can still be entropy produced by continuously mixing the fluid inside the cell. In the case that the specific entropy at inlet and inside the cell are not equal, the last term in the equation does not reduce to zero. This occurs if the temperatures are not equal because the specific entropy depends on pressure and temperature.

$$\dot{S}_{prod}^M = m \frac{ds}{dt} - \dot{m}_{in} (s_{in} - s) \quad (5)$$

Each fluid cell emits a heat flow  $\dot{Q}$  at the heat port with the temperature  $T_{hp}$ . This flow conveys entropy that can be determined by the following equation.

$$\dot{S}_Q = \frac{\dot{Q}}{T_{hp}} \quad (6)$$

Before being emitted, the heat flow is transferred from the medium inside the cell (temperature  $T$ ) to the heat port (temperature  $T_{hp}$ ). The temperature gradient between  $T_{hp}$  and  $T$  is determined by the heat transfer relation and the heat transfer coefficient. In the cell model, the equations for the heat transfer phenomena are implemented. This heat transfer causes entropy production, which can be determined according to [Bejan88] as follows.

$$\dot{S}_{prod}^Q = \frac{\dot{Q}}{T} - \frac{\dot{Q}}{T_{hp}} \quad (7)$$

Pressure drop between the inlet and outlet port also leads to entropy production. It can be determined as presented in [Bejan88].

$$\dot{S}_{prod}^{\Delta p} = \dot{m} \int_{out}^{in} \frac{v}{T} \Big|_{h=const} dp \quad (8)$$

This formula can be linearized

$$\dot{S}_{prod}^{\Delta p} = \dot{m} \frac{v}{T} \Delta p \quad (9)$$

$\Delta p$  represents the pressure drop.

Equation 1 has to be adapted for the determination of the entropy production inside a **wall cell**. Since there is no medium flowing through the wall cell, there are no terms for entropy transportation via mass flow, and no pressure drop occurs. The entropy production due to the modeling of the wall cell can be determined according to the following equation:

$$\dot{S}_{prod}^M = m \frac{ds}{dt} - \dot{S}_Q - \dot{S}_{prod}^Q \quad (10)$$

Heat can be emitted at each of the heat ports  $i$  with the overall entropy conveyed because of heat flow being  $\dot{S}_Q = \sum_{i=1}^n \dot{S}_{Q,i}$ . Each of the summands  $\dot{S}_{Q,i}$  can be determined according to equation 6. The heat transfer from the medium inside the cell to one heat port or vice versa causes entropy production. Each production term  $\dot{S}_{prod,i}^Q$  can be determined in accordance with equation 7 and has to be summed in order to determine the overall entropy production due to heat transfer,  $\dot{S}_{prod}^Q = \sum_{i=1}^n \dot{S}_{prod,i}^Q$ .

The entropy production resulting from modeling assumptions  $\dot{S}_{prod}^M$  (see equation 10) represents only small numerical errors. There is no mixing inside the wall cell and the term  $\dot{S}_{prod}^M$  can be neglected.

In order to calculate the entropy production due to each effect for the whole tube, the results of the entropy production in the cells are summed. The results of the refrigerant and the liquid tube are then summarized to determine the entropy produced within the whole heat exchanger.

### 3.2 Valve

In the valve model (control valve) the refrigerant is throttled adiabatically. It is assumed that the kinetic energy of the flowing refrigerant is completely dissipated. Since the valve has been modeled as a component without volume, the second law for the valve has to be applied in the steady state form.

$$\sum_{i=1}^n \dot{m}_i s_i + \dot{S}_{prod}^T = 0 \quad (11)$$

As the mass flow rate  $\dot{m}_i$  and the specific entropy  $s_i$  at the inlet and outlet ports are known, this equation is used to determine the overall produced entropy.

$$\dot{S}_{prod}^T = - \sum_{i=1}^n \dot{m}_i s_i \quad (12)$$

### 3.3 Compressor

The compressor model is based on an efficiency model with isentropic, volumetric and effective isentropic efficiency. Furthermore, a heat flow from the housing surface to the surroundings is considered, but is set to zero in the simulation. The main entropy production in the compressor is caused by the following loss mechanisms, which result from the compression process of a reciprocating type compressor. These are: friction losses due to mechanical components such as pistons and piston rings and swash plate, throttling losses that take place in the valves, flow channels and chambers, the heat transfer between the different compressor components, e. g. the suction and discharge chamber, the leakage losses and losses caused by the control valve. Since the compressor is modeled as a volumeless component, the second law for the compressor has to be applied in steady state form:

$$\sum_{i=1}^n \dot{m}_i s_i + \dot{S}_Q + \dot{S}_{prod}^T = 0 \quad (13)$$

$\dot{S}_Q$  specifies the entropy flow that is discharged with the heat flow.

### 3.4 Ejector

When a medium is throttled in a conventional valve, friction losses occur and the kinetic energy of the medium is completely dissipated. In an ejector, however, the kinetic energy of a primary flow at high pressure can be partly used to compress a secondary flow and thus to diminish the compression work done in the compressor. Figure 3 illustrates the functionality of an ejector.

The driving flow exits the driving nozzle with a high velocity and carries with it a flow from the suction nozzle. Since the cross section of the suction nozzle becomes progressively narrower, the suction flow is accelerated and the pressure drops. Both the suction and driving flows exchange momentum, are mixed in the mixing tube and flow through a diffuser before leaving the ejector. The pressure inside the diffuser increases with decreasing velocity.

The ejector is modeled using an analogous model consisting of several separate components. Because

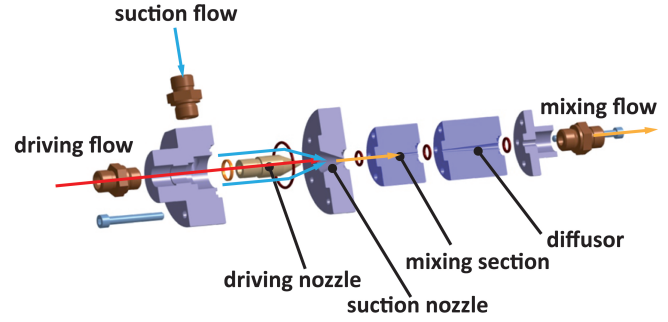


Figure 3: Exploded view of an ejector

the exchange of momentum is not ideal and entropy will be produced, the ejector can partly recover the kinetic energy. However, the entropy produced has not been determined in detail for this work. A simplified approach has been used instead, and the entropy production rate for steady state has been determined as the difference between inlet and outlet entropy flow rates according to the second law in steady state.

$$\dot{S}_{prod}^T = - \sum_{i=1}^n \dot{m}_i s_i \quad (14)$$

### 3.5 Separator

The separator model is similar to the refrigerant cell model apart from the fact that no heat transfer or pressure loss is considered, and that the refrigerant is not mixed, but separated into liquid and gaseous phase. The entropy production rate is determined by the following equation.

$$\dot{S}_{prod}^T = m \frac{ds}{dt} - \sum_{i=1}^n \dot{m}_i s_i \quad (15)$$

As there are no effects producing entropy  $\dot{S}_{prod}^T$  is equal to zero.

### 3.6 Implementation of Entropy Production in TIL

In the Modelica library TIL, the specific entropy  $s$  is implemented as a function of  $p$  and  $h$ . In order to reduce the index of the differential algebraic equation system, the terms in the entropy equation have to be expressed by means of state variables used for the description of the system. This implies that the term  $\frac{ds}{dt}$  (derivative of the specific entropy with respect to time) had to be rewritten in terms of  $p$  and  $h$ . To transform the equation Bridgeman tables, which can

be found in [Bejan88] were used. This made the implementation more numerically effective by not relying on Dymola for the rearrangement of the equation system. The discussed mathematical equations to determine the entropy production were implemented in each model. The collection of the results in the summary records simplifies the readout by other programs used to analyze the results.

## 4 Visually Supported Analysis of Simulation Results

The simulation results were analyzed with the help of 2d-plots which show the temperature relations, and Sankey diagrams which show the entropy flow beside the production rates. Therefore the entropy flows at the inlet and outlet port of each component were determined. The entropy production caused by heat transfer, pressure drop, numerical errors due to modeling and the overall entropy production were calculated according to the aforementioned equations and illustrated by bar charts. The visualized entropy flows were normalized for each medium such that the flow with the lowest specific entropy is equal to zero. With the help of the Sankey diagrams, the entropy shift within the flows is visualized, and for each medium the relation of the entropy flows between the components becomes clear. Sankey diagrams are a powerful visualization method to analyze all kind of flows. A detailed discussion of the application of Sankey diagrams can be found in [Schmidt06].

### 4.1 Entropy Production in Heat Exchangers

The diagrams in figures 4 and 5 illustrate the temperature curves in the gas cooler (R744) and the condenser (R134a) of a steady-state ejector refrigeration cycle for domestic hot water. It can be clearly seen that the temperature glide in the gas cooler (R744) leads to a lower mean driving temperature difference in the gas cooler than in the condenser (R134a). In the evaporators, the refrigerant is evaporated at a nearly constant temperature and exits the heat exchangers with low superheating, which is controlled by the controller. This results in a lower mean driving temperature difference and lower entropy production due to heat transfer in the evaporators. See figure 7 and 9 for entropy production in the evaporators in relation to entropy production in the gas cooler / condenser. In figure 6 the profile of entropy production due to different effects is illustrated for the cells of the gas cooler. The cor-

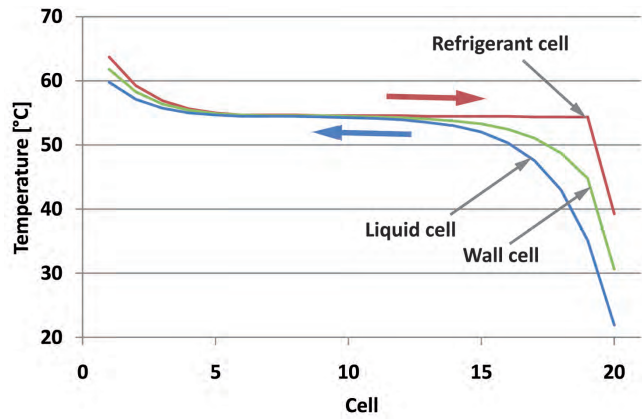


Figure 4: Temperature profile of refrigerant, liquid and wall cells inside the condenser (R134a domestic hot water)

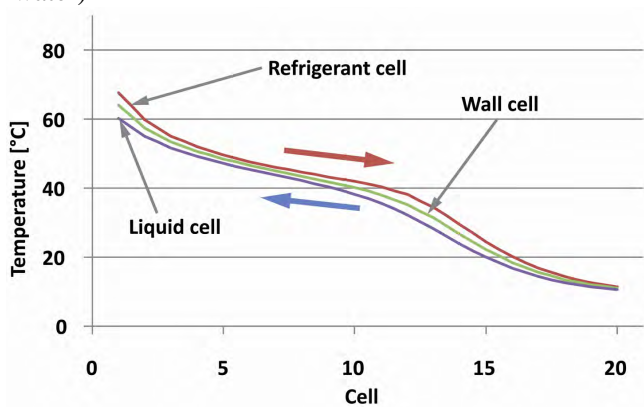


Figure 5: Temperature profile of refrigerant, liquid and wall cells inside the gas cooler (R744 domestic hot water)

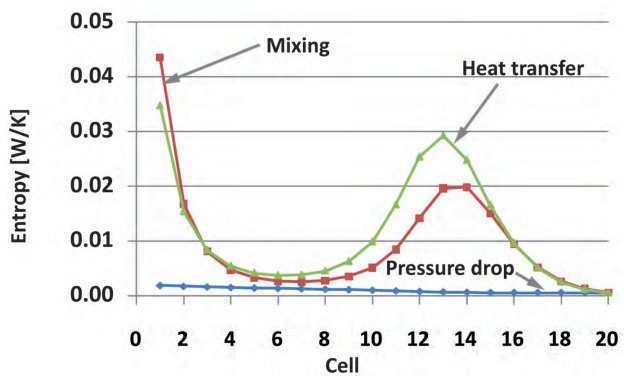


Figure 6: Profile of entropy production inside the gas-cooler (R744 domestic hot water)

responding temperature profile is shown in figure 5. Wherever high temperature differences occur, the produced entropy due to heat transfer and mixing (modeling assumption) is high. The entropy production rate due to pressure drop is low in comparison to the production rate due to heat transfer and mixing.

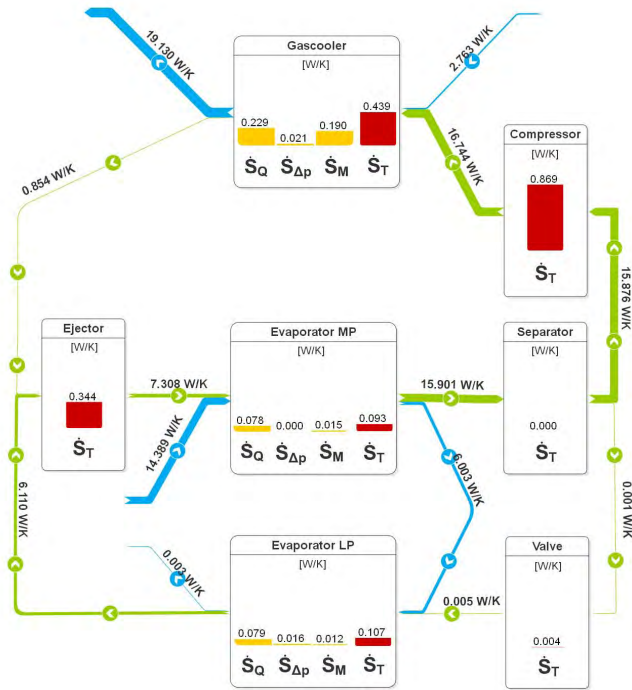


Figure 7: Entropy flow and production rate in an R744 heat pump cycle used to heat up hot domestic water. Entropy production rate due to heat transfer ( $\dot{S}_Q$ ), pressure drop ( $\dot{S}_{\Delta p}$ ), modeling ( $\dot{S}_M$ ) and total entropy production rate ( $\dot{S}_T$ ) for each component are represented by bar charts. The entropy flow is normalized to the lowest specific entropy of each medium. Entropy production and flows are represented in different scales.

#### 4.2 Comparison R744 ejector cycle for domestic hot water and floor heating

The figures 7 and 8 show the Sankey diagrams of a steady state R744 ejector refrigeration cycle for domestic hot water and floor heating operation respectively. First, looking at the gas cooler, it is shown that the entropy production caused by heat transfer in the case of floor heating operation is higher than in the case of domestic hot water operation. This is due to the higher driving temperature difference in the gas cooler in the floor heating operation. However, the entropy production caused by mixing (modeling assumption) in the case of floor heating operation is lower than in the case of domestic hot water operation, despite the greater refrigerant and water mass flow rates. The reason for this is the lower temperature gradients between the inlet and outlet of the refrigerant as well as liquid tubes. With the heating capacities equal in both the floor heating and domestic hot water operation modes, in the floor heating mode, the compressor and the ejector produce more entropy, although the water mass

flow rate and the refrigerant mass flow rate are greater. That shows that the R744 ejector refrigeration cycle is better suited to heat water up to higher temperatures.

#### 4.3 Comparison R744 and R134a Ejector Cycle for Domestic Hot Water

The Sankey diagrams of a steady state R744 and R134a ejector refrigeration cycle for domestic hot water mode are illustrated in figure 7 and 9. The results show that entropy production caused by heat transfer in the condenser (R134a) is significantly higher than in the gas cooler (R744). This is due to the higher mean driving temperature difference between the refrigerant and the water in the condenser. The temperature curves in the condenser and the gas cooler are illustrated in figure 4 and 5. Because of the temperature glide in the gas cooler, the mean driving temperature difference is lower. For the same reason, the entropy production resulting from mixing (modeling assumption) is also higher in the condenser. In the R744 refrigeration cycle, production of entropy in the compressor and ejector is higher, the reason for this being the different refrigerant properties and process controls. Because of this, the pressure difference between the high and low pressure level in the R744 refrigeration cycle is higher. An ejector heat pump using R744 as refrigerant is suited to supply domestic hot water better than a heat pump using R134a, if particular attention is directed to the entropy production in the condenser or gas cooler. In addition, the energy saving potential with an ejector is higher in an R744 cycle than in an R134a cycle.

### 5 Conclusions and Outlook

The presented work shows how an analysis of the dissipation effects in thermodynamic systems can be done with the help of simulation. For this purpose the equations are presented which are needed to mathematically describe the observed entropy-producing phenomena. In particular, the entropy production in the heat exchangers is examined. Entropy production resulting from heat transfer, pressure drop and numerical error due to modeling are observed. Using the example of an ejector heat pump, it is shown how the resulting simulated entropy production can be visualized and used in the dissipation analysis. The analysis is carried out using bar diagrams, Sankey diagrams and 2d-plots. Heat pumps using R134a and R744 were compared for both domestic water heating and floor

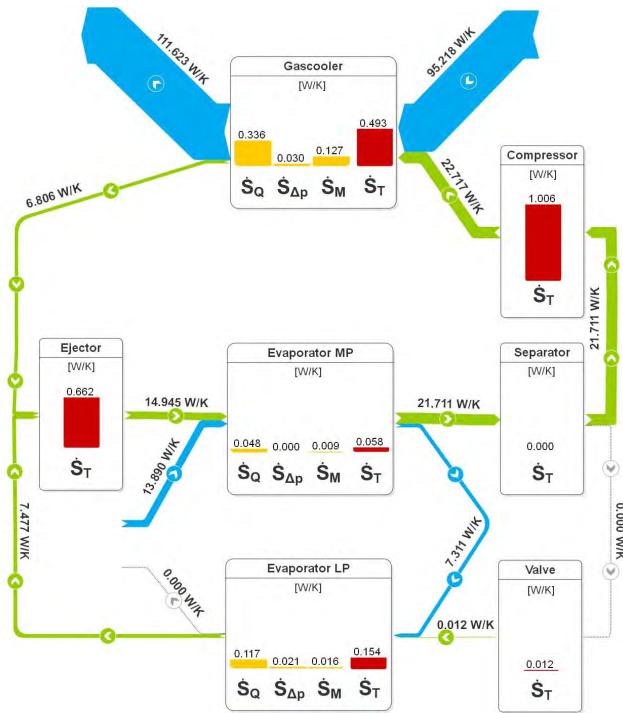


Figure 8: Entropy flow and production rate in an R744 heat pump cycle used to heat water for floor heating.

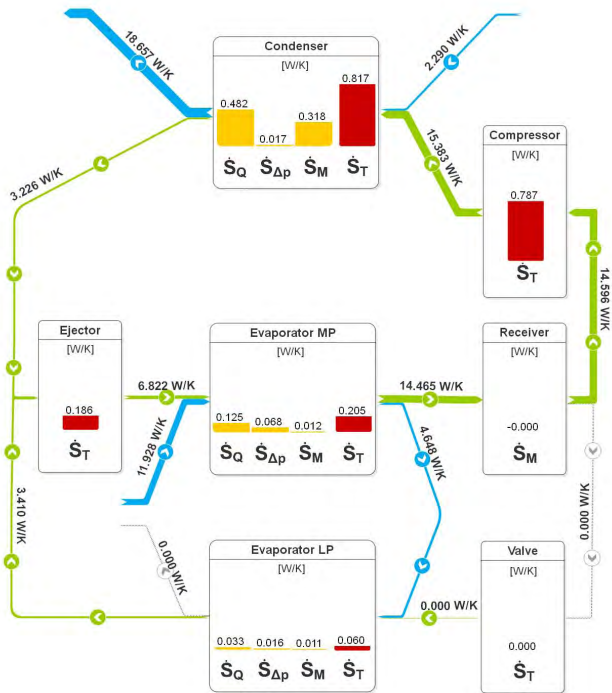


Figure 9: Entropy flow and production rate in a R134a heat pump cycle used to heat domestic hot water.

heating. The investigation shows that the heat pump with R744 is better suited for domestic hot water operation. It is shown that this analysis method is suitable for investigation of thermodynamic systems on the basis of entropy production. In the future, it is planned

to research whether the boundaries of the system can be altered to produce an even better analysis or not. In addition, it is planned to carry out a more detailed analysis of entropy production within the ejector model.

## References

[Baumann06] Baumann W., Bunge U., Fredrich O., Schatz M., Thiele F. Finite-Volumen-Methode in der Numerischen Thermofluidodynamik. Technische Universität Berlin, Institut für Strömungsmechanik und technische Akustik: Vorlesungsmanuskript, Berlin, 2006.

[Bejan88] Bejan A. Advanced Engineering Thermodynamics. John Wiley & Sons, New York, 1988.

[Bejan02] Bejan A. Fundamentals of Exergy Analysis, Entropy Generation Minimization, and the Generation of Flow Architecture. In: International Journal of Energy Research vol.26 no.7 p.545-565, 2002.

[Cerbe07] Cerbe G., Wilhelms, G. Technische Thermodynamik, Hanser Verlag, München, 2007.

[Elbel06] Elbel S., Hrnjak P. Development of a Prototype Refrigerant Ejector used as Expansion Device in a Transcritical CO<sub>2</sub> System, Presentation VDA Alternative Refrigerant Winter Meeting Saalfelden, 2006.

[Franke04] Franke U. Thermodynamische Prozessanalyse: Ursachen und Folgen der Irreversibilität. Shaker, Aachen, 2004.

[Patankar80] Patankar S. Numerical Heat Transfer and Fluid Flow. Hemisphere Publ. Co, New York, 1980.

[Richter08] Richter C. Proposal of New Object-Oriented Equation-Based Model Libraries for Thermodynamic systems. Braunschweig, Germany: PhD Thesis, Department of Mechanical Engineering, Institute of Thermodynamics, TU Braunschweig, 2008.

[Schmidt06] Schmidt M. Der Einsatz von Sankey-Diagrammen im Stoffstrommanagement. Beiträge der Hochschule Pforzheim, Nr. 124, Pforzheim, 2006.